Semiconductor Physics, Quantum Electronics & Optoelectronics, 2013. V. 16, N 3. P. 273-279.

PACS 64.70.K-, 78.60.Lc

8H-, 10H-, 14H-SiC formation in 6H-3C silicon carbide phase transitions

S.I. Vlaskina[1,2], G.N. Mishinova[3], V.I. Vlaskin[4], V.E. Rodionov[1], G.S. Svechnikov[1]
[1]*Institute of Semiconductor Physics, National Academy of Science of Ukraine*
45, prospect Nauky, 03028 Kyiv, Ukraine; e-mail: businkaa@mail.ru
[2]*Yeoju Institute of Technology, 200 Myeongseong-ro, Gyeonggi-do, 469-705 Korea*
[3]*Taras Shevchenko Kyiv National University, 64, Volodymyrska str., Kyiv 03033, Ukraine*
[4]*Sensartech, 2540 Lobelia Dr., Oxnard, 93036 California, USA*

Abstract. In this paper the results of photoluminescence researches devoted to phase transitions in 6H-3C-SiC have been presented. High pure 6H-SiC crystals grown by Tairov's method with and without polytype joint before and after plastic deformation at high temperature annealing were investigated using optical spectroscopy. Low temperature photoluminescence changes in the transition phase of SiC crystal represented with the stalking fault spectra within the temperature range 4.2 to 35 K. The stalking fault spectra indicate formation of metastable nanostructures in SiC crystals ($14H_1$ ⟨4334⟩, $10H_2$ ⟨55⟩, $14H_2$ ⟨77⟩). The phononless part of each stalking fault spectrum consists of two components of radiative recombination that are responsible for hexagonal and cubic arrangement of atoms. Each of radiative recombination components in the stalking fault spectrum has the width of entire band 34 meV and shifts relative to each other by 26 meV. The overlap area of those components equals to 8 meV. The super-fine structure of the recombination components in spectrum is observed, and it is related to different Si – Si or C – C and Si – C bonds. Behavior of all the stalking fault spectra is similar (temperature, decay of luminescence). The processes of the phase transition are explained by the mechanism of interfacial rearrangements in the SiC crystals.

Keywords: silicon carbide, polytype, stacking fault, nanoparticle, phase transitions.

Manuscript received 10.06.13; revised version received 26.07.13; accepted for publication 19.09.13; published online 30.09.13.

1. Introduction

Researches associated with formation of polytype structures are a staple of modern condensed matter physics of nanostructures. The phenomenon of polytypism is inherent to single crystals, films, powders, polycrystalline compact materials, and nanostructures. Polytypes of SiC differ fundamentally only by the number and the sequence of position of the atomic Si – C bilayers relative to the adjacent (neighboring) bilayers in a cubic (c) or hexagonal (h) arrangements. Replacement of any layer in the cubic setting on a hexagonal (or vice versa) can be viewed as a stacking fault (SF) of the polytype, which has a strictly defined motif of alternating atomic planes, the so-called zig-zag chains. Regular input of h-layers in a cubic structure 3C-SiC (β-phase) can give structure of the α-phase (H or R).

In terms of the dislocation, the transition mechanism of the cubic structure to the hexagonal structure is discussed in the articles [1-7]. In terms of formation of the multilayers polytypes, transition of the hexagonal structure to the cubic one is discussed in [8-13]. The interface interactions between 3C-SiC and 2H-SiC have been also investigated [14]. The mechanism of this transition is the object of various simulations [15, 16].

Also, SiC polytypes can be described by different stacking of Si – C layers that are perpendicular to the direction of the SiC closed-packed plane. SF play the main role in the process of structure transformation [11, 13]. SF dimension of a few SiC lattices is a quantum well 3C-SiC within wider band-gap α-SiC. The structure leads to appearance of the quantum effects and SiC actually becomes a direct band gap semiconductor, which results in intense photoluminescence in the blue part of the spectrum. A new type of heterostructure can be created using SiC, namely: heterostructure not between different materials but between different modifications of the same material [17]. Degradation of the electrical characteristics of bipolar SiC devices is explained by the presence of SF in crystal bulk [18, 19]. Formation of different polytypes under the same thermodynamic conditions can be understood when using optical spectroscopy analysis [1, 20].

This work is aimed at properties of high purity 6H-SiC crystals (before and after plastic deformation and high temperature annealing treatment) and disordered grown layers in the crystals of α-SiC (mainly 6H-SiC) by using optical spectroscopy such as low temperature photoluminescence (LTPL), Photoluminescence excitation spectra (PES) and absorption spectra have been analyzed.

2. Experiment

The luminescence spectra were obtained using excitation by the mercury lamp (λ = 365 nm), and by lasers: nitrogen laser (λ = 337 nm); He-Cd laser (λ = 441.6 nm); Ar-laser (λ = 488 nm).

Crystals were grown by sublimation (Lely method), were selected according to the phase composition (α- or β-phase) and the degree of structural disorder (control, twinning, and one-dimensional disorder). Crystal structural researches were carried out using X-ray diffraction (Laue method) and electron diffraction methods. Thermal treatment of crystals (high-temperature annealing) was performed in a resistance furnace with a graphite heater in argon atmosphere at T = 2000…2100 °C for 1 to 10 hours. Plastic deformation of the samples was carried out in a resistance furnace at the argon atmosphere by three points bending at 2000 °C for 15…30 min.

2.1. 6H-SiC perfect crystals

High purity crystals with a very low concentration of impurities have been selected for the spectroscopic investigation of the phase transition 6H-3C SiC. Laue diffraction patterns indicated a single-phase crystal composition. Normally, only in such perfect crystals of 6H-SiC observed is the well known spectrum of exciton impurity (nitrogen) complexes (as known as PRS) together with ABC-spectra associated with titanium. The spectra of LTPL of the crystal (at 4.2 K) with the non-compensated nitrogen concentration $N_D - N_A \sim (6…7) \cdot 10^{16}$ cm^{-3} were investigated. The change of the LTPL spectra had been observed after plastic deformation at the temperature from 2000 up to 2100 °C for 30 min in argon atmosphere. A fine spectrum structure of the SiC appeared. Similar results in SiC crystal after annealing were demonstrated and specified as SF in Refs. [1, 9, 13].

The intensity of the PRS and ABC maxima is considerably reduced after applying the force to the crystals. The plastic deformation stimulates an emergence of the so-called L-spectrum, which is associated with presence of vacancies, and it was previously obtained only by the ion bombardment of crystals. This confirms a possibility of vacancies formation during the process.

2.2. Grown polytype's transformations in SiC crystals

For better understanding the process of transformation the pure SiC crystals ($N_D - N_A \sim (4…9) \cdot 10^{16}$ cm^{-3}) with natural inter-grown SiC polytype's joints were specially selected. The crystals have been studied in detail for the presence of similar spectra. Crystal structure of disordered layers was determined by diffuse smearing of reflections in Laue pattern. The "twin plates" of the β-phase in SiC (10…100 Å lamellae) and the basic structures of the α-phase: 6H-SiC, 15R-SiC, 21R-SiC were investigated. Fig. 1 shows LTPL of various samples of the inter-grown polytypes at T =4.2 K. The overall spectral pattern of each sample represents a specific series of spectra SF_1 (Fig. 1a), SF_2 (Fig. 1a, c), SF_3 (Fig. 1a, b), SF_4 (Fig. 1b) which look like spectra of the 6H-SiC crystal after applying the force.

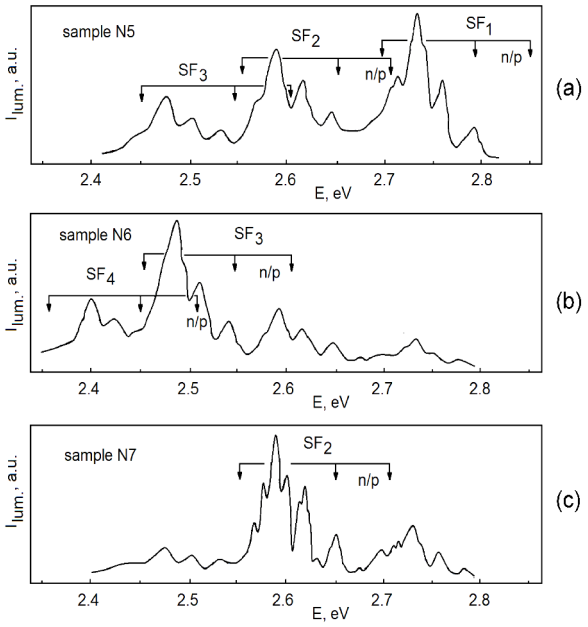

Fig. 1. LTPL at 4.2 K of the inter-grown polytypes joint in different samples: (a) sample N5; (b) sample N6; (c) sample N7.

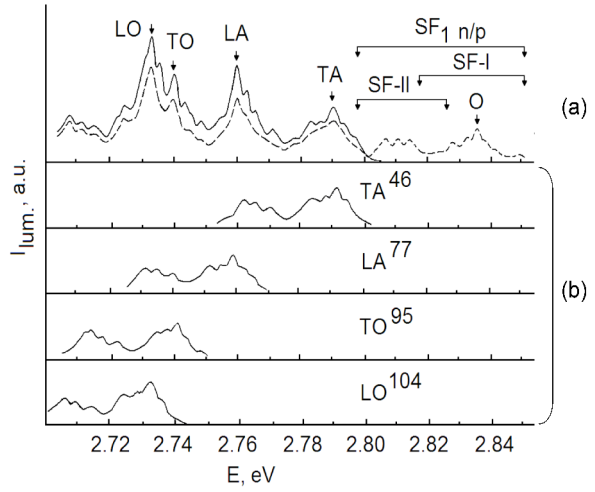

Fig. 2. SF_1 spectrum of SiC at 4.2 K: (a) reconstituted phononless part of SF_1 spectrum; (b) phonons in SiC involved in SF_1 spectrum.

The difference is that all the SF fine spectra are located at the different energy scale with different intensities of the spectra. But a comprehensive spectroscopic analysis showed that all SF spectra have the same characteristics and principle of their construction regardless of placement in the common energy scale. Transcript structure of the spectrum SF_i (where $i = 1, 2, 3, 4$) is made with the spectrum SF_1 that is most frequently observed. Transcripts of another SF_i fine spectrum are the same. Other SF_i spectra are located in different energy region compare with SF_1 fine spectra.

The entire structure of the spectrum SF (Fig. 2a) can be obtained by summing together additive phonon replicas to some phononless part of the spectrum (Fig. 2b).

Phonons of extended edge Brillouin zone of the silicon carbide ($E_{TA} = 46$ meV, $E_{LA} = 77$ meV, $E_{TO} = 95$ meV, $E_{LO} = 104$ meV) are involved in the emission. Adding the phonon replicas spectrum to the proposed phononless structure spectrum gives the photoluminescence spectrum (LTPL) (Fig. 2a). By the way, a specific feature is that the phononless part itself is not observed. The phononless part of fine spectra was created in accordance with the structure of TA-replica and its transitions as a whole to higher energies by the energy of TA phonon (46 meV). Fig. 3 shows that the phononless spectrum of SF_1 is located within the energy region (2.853…2.793 eV) with the width of the entire band 60 meV. The energy region for SF – I spectrum is 2.853…2.819 eV and for SF – II spectrum is 2.827…2.793 eV, accordingly.

It turns out that, after determining the position of the phononless part of SF_1 in the energy scale, the energy of the short-wave spectrum SF_1 is the same as the exciton band gap of the SiC-polytype 21R-SiC at $T = 4.2$ K, and equal to 2.853 eV [1]. The energy of inserting a 2H(3C) crystal in a 3C(2H) matrix had been calculated and is 68.4 meV/atom for (2H), and 66.9 meV/atom for (3C) [14]. Both calculated energy values are about the same as the energy obtained from a width of the entire band of SF_i spectra (60 meV).

Careful investigation of phononless part of the SF_1 showed that the spectrum by itself consists of two components are SF – I (2.853…2.819 eV) and SF – II (2.827…2.793 eV). Each of them has the width of the entire band 34 meV. Maximums of SF – I and SF – II are shifted relatively to each other by 26 meV (Fig. 4). The overlap spectrum area equals to 8 meV.

Two parts of the SF_i (SF – I and SF – II) spectrum also have super-fine structure. Resolution of the super-fine structure SF – I and SF – II is different in the case of different natural inter-grown SiC crystal polytypes. The smallest width at half maximum of the fine structure SF – I and SF – II components is 1.5 meV. According to Ref. [14], the process of interface formation in the SiC crystal requires energy 0.151 eV/Å^2. This energy induces distortion of tetrahedrons and generates compressed Si – Si and stretched C – C bonds. So, the super-fine structures of SF – I and SF – II can be caused by the arrangement of each atom.

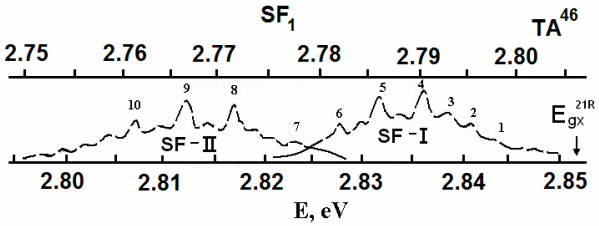

Fig. 3. The phononless part of the SF_1 spectrum.

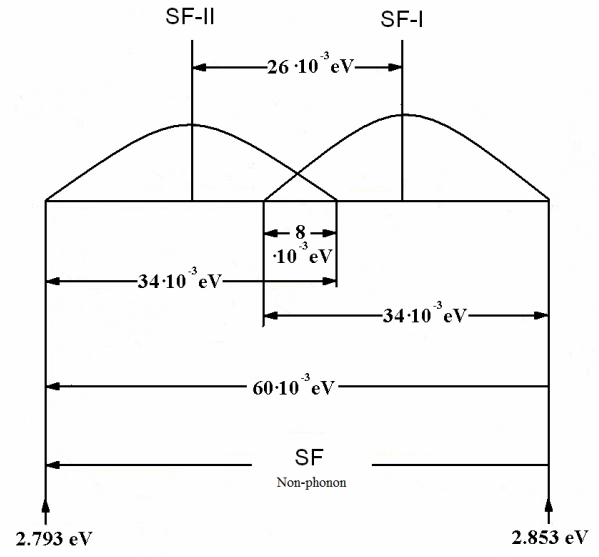

Fig. 4. Scheme of the phononless spectrum SF_1.

3. Discussion

Silicon carbide is a covalent crystal in which atoms have sp^3-type hybridization. The covalent bonds between atoms with sp^3-type of hybridization can explain polytypism in SiC. If a cubic crystal to orient along the crystallographic direction (111) and hexagonal and rhombohedra crystals along the (0001), the crystal of silicon carbide can be considered as a layered macro-molecular one (like cyclohexane).

Cubic crystal 3C-SiC is characterized by the interlayer structures like "N". Hexagonal 2H polytype layers are linked like "V" structures. The structure of another hexagonal and rhombohedra polytypes is determined by sequence of "N" and "V" structures along the (0001) direction. The difference of a crystal structure of the silicon carbide polytypes is only in a nature of the interlayer bond, but structure of each layer is exactly the same.

From the fact that the energy of bonds between atoms in the cubic 3C-SiC (cubic arrangement) are not identical to the energy of bonds between atoms in hexagonal 2H-SiC (hexagonal arrangement), it implies the assumption why SF_i spectrum has two parts SF – I and SF – II. Namely, the difference in the interlayer bond's energies at the exactly same structure of each layer gives appearance of the super-fine structure of SF – I and SF – II parts in every spectrum.

These differences of the energy scale of SF – I and SF – II should be attributed to particular inter-atomic bonds. The phononless part of the SF – I spectrum consists of the components of radiative recombination, which is responsible for hexagonal and in the case of SF – II for cubic arrangements of atoms.

The same character of all the SF_i spectra is confirmed by the same temperature behavior. Both of the SF_i spectra are observed at the temperatures 4.2 up to 35 K (Fig. 5). The parts SF – I are observed at 4.2…18 K (Fig. 5a), and SF – II – at 4.2…35 K, accordingly (Fig. 5a, b). Fig. 5a illustrates the sequence decay of short-wave maximums for SF – I and SF – II (shown above in Fig. 3). At the temperatures higher than 18 K, the sequence decay of short-wave maximums associated with SF – II remains only (Fig. 5c). The thermal activation energy of the SF – I and SF – II parts is different and equal $E_a^T \approx 3.5\,\text{meV}$ and $E_a^T \approx 7.5\,\text{meV}$, accordingly (Fig. 5b).

The dependence of PL intensity with the intensity of exciting light has sub-linear character, namely: $I_{PL} = I^{\alpha}_{\text{exc.light}}$, $\alpha = 0.7$. At the same time, significant duration of the PL decay is observed. The PL intensity of the SF_1 spectra is registered after switching-off the excitation and has the delay time $3\cdot10^{-3}$ s herewith $I_{PL} = 0.02 I_0$. The intensity of the SF – I part decays rapidly. All these allow to make an assumption of possibility that there is a saturation effect of the radiation centers as well as the fact that recombined electrons and holes are significantly separated in space with the weak overlap of wave functions. High-temperature annealing (T = 2000 °C, t = 5 h) of pure SiC crystals (with SF) leads to a weakening the short-wave SF_i maximums.

In the beginning SF – I component disappears in all SF_i spectra (Fig. 3, curves 1 to 5), then the SF – II one disappears (Fig. 3, curves 7 to 10). After the high-temperature annealing for more than 5 hours, the SF – I components of spectra completely disappear. For better understanding the location of SF – I in the PL spectrum one, needs to study the overlap in PL spectra for SiC before (Fig. 6a, curve 1) and after deformation (Fig. 6a, curve 2).

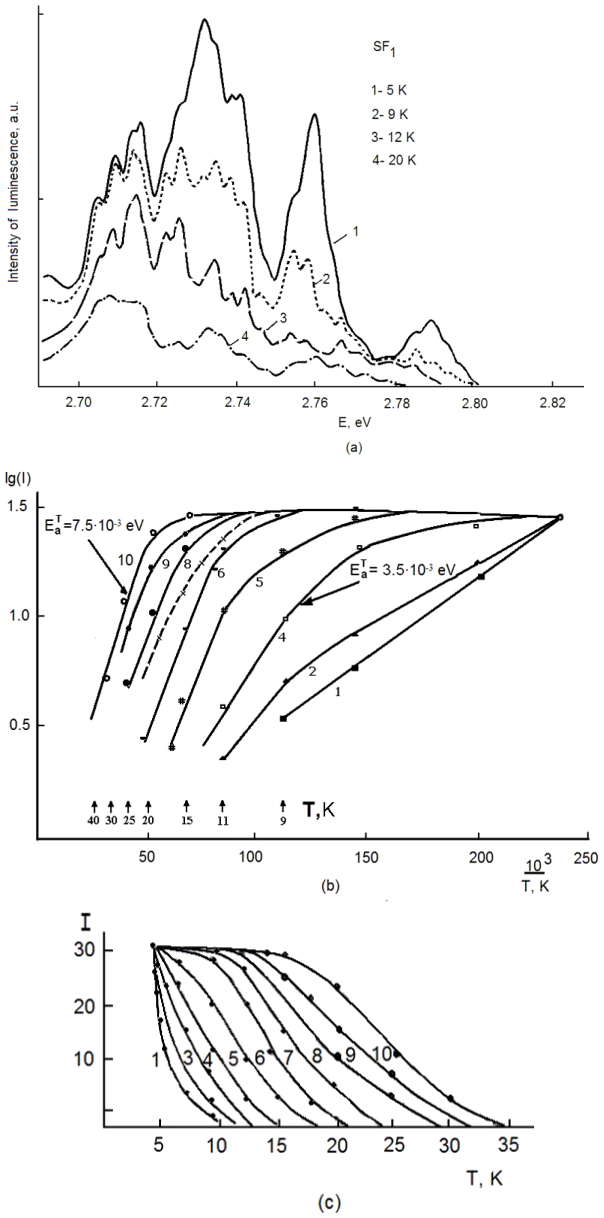

Fig. 5. Temperature behavior of the SF_1 spectrum for the sample N5: (a) SF_1 spectrum at various temperatures; (b) dependence of the PL intensity for the fine structure with inverse temperature; (c) temperature dependence of the PL intensity of the fine structure.

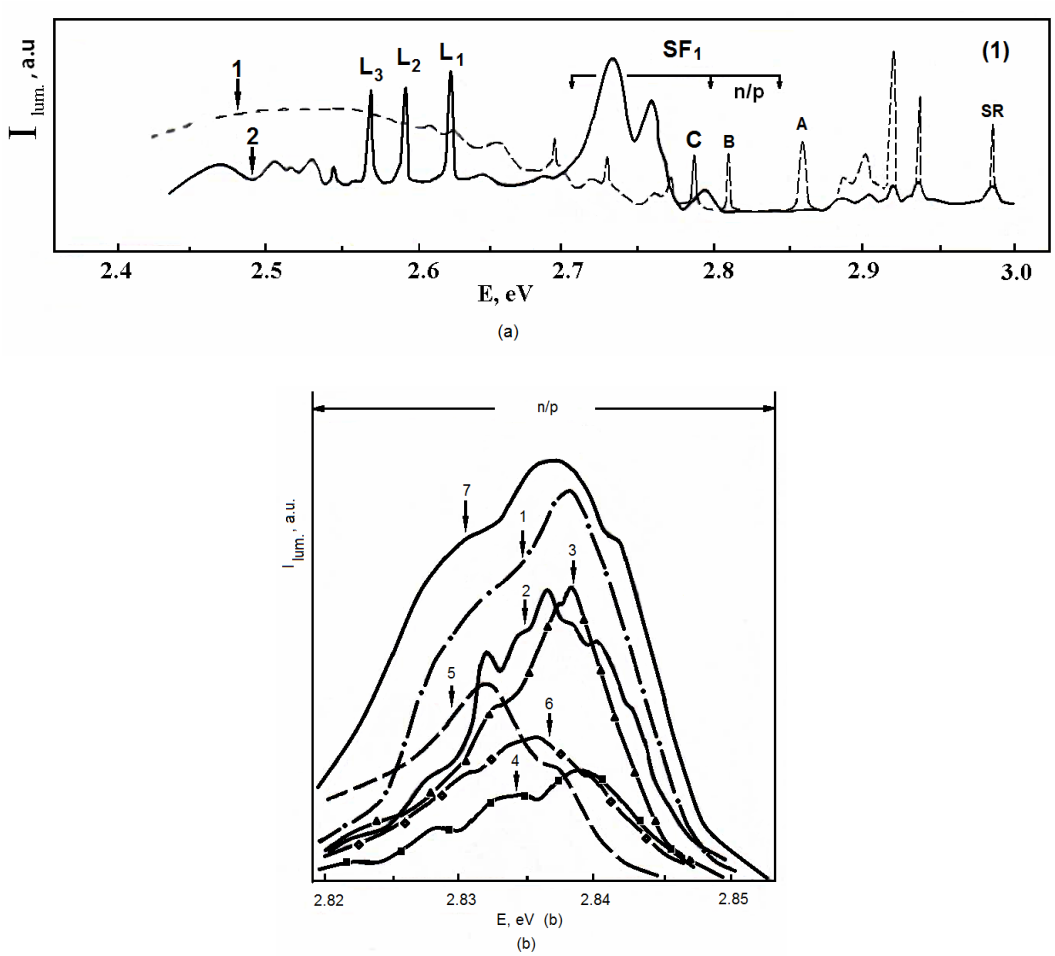

Fig. 6. LTPL spectra of SiC crystals: (a) pure 6H SiC before and after plastic deformation; (b) intensity of the fine structure SF-I component in SF_i spectra of as-grown crystal polytype's joint and after plastic deformation by pressure.

The phononless part of SF_1 spectra was obtained by calculation and is located between 2.793 and 2.852 eV (Fig. 6a). Variation of changes in the distribution of intensities inherent to the phononless part of the fine SiC spectra is shown in Fig. 6b. The curves 1 and 2 in Fig. 6b show the spectroscopic features of the two different samples of SiC growth polytype's joint. After plastic deformation of the non-defect SiC crystal (Fig. 6a, curve 1) by applying the force along c-axis, the SF – I spectrum appears (Fig. 6b, curve 3). The appearance of the SF – I spectrum due to various external influences on the crystal is as follows: curve 4 (for the high force), curve 5 (for the low force), curve 6 (for additional applied forces). Curve 7 is the intensity distribution of $\beta \rightarrow \alpha$ transformation in the β-SiC after the high temperature annealing at $T = 2000\ldots2100$ °C. All these spectra emphasizes the complex structure of the SF – I spectrum and confirm the association with the peculiarities of structural states of the crystals. The super-fine structure of SF – I component is related with the bond length between atoms in polytypes and depends on the crystallographic direction [21].

In order to understand the origin of super-fine structure in the spectrum, it needs to review the faulted-arrangement structure properties of different hexagonal layers in the SiC polytypes.

SiC polytypes have varying degrees of hexagonality, and the numeric value of which is defined as a ratio of amount of the atoms in the hexagonal arrangement and total amount of atoms in the polytype's cell. Similar phenomena were obtained in diamond and have a linear character of dependence of the interlayer distances with the degree of hexagonality [22]. The relationship of the degree of hexagonality and optical band gap in the SiC polytypes is linear [1]. By plotting the short-wave edge of each SF_i spectra on the energy scale and the corresponding excitation spectra in the dependence of the percentage hexagonality in the different polytypes, percentage of new hexagonality nanostructures can be obtained. The metastable form of nano-structures appear either in the growth process or after plastic deformation.

Short-wave edge location of the phononless part for each of the SF_i spectra is an indicator of the nanopolytype junction [23]. The locations of the spectrum the phononless parts of SF_i in the energy scale are summarized in Table.

Table. The phononless part of SF as indicator of formation of metastable intermediate phase.

Stacking fault	Locations (eV)	Polytype	Hexagonality (%)
SF_1	2.853	14 H_1 ⟨4334⟩	28.5
SF_2	2.712	$10H_2$ ⟨55⟩	20
SF_3	2.611	$14H_2$ ⟨77⟩	14.3
SF_4	2.515	N/A	7
SF_5	3.002	33R ⟨$(3332)_3$⟩	37
SF_6	2.78	8H ⟨44⟩	25

After determining the position of the spectrum for the SF_1 phononless part in the energy scale, it turned out that the short-wave part of the spectrum is the same to the position of the exciton band gap polytype 21R at T = 4.2 K, i.e. 2.853 eV.

The study of the excitation spectra gives better understanding the total complex panorama of the PL spectrum (SFs). Each SFs has its own spectrum of excitation. The total excitation spectrum repeats the absorption spectra. The linear dependence of the exciton band gap (E_{gx}) with a percentage of hexagonality of polytypes indicates occurrence of a nanostructure.

If the initial polytypes were 15R ⟨$(23)_3$⟩ and 6H ⟨33⟩, then the spectrum of SF_5 was observed. Due to the overlap with the other spectra, the SF_4 spectrum is difficult to determine. SF_4 corresponds to the unknown polytypes with lower percentage of hexagonality (up to 7%). The SF_6 had overlap with another spectrum and may correspond to the polytype 8H ⟨44⟩.

The possibility of occuring such new nano-phase with the percentage hexagonality less than 25% (both in the growth and in the result of solid state transformations) was confirmed by high-resolution electron microscopy [24, 25] and by first-principle study of 8H-, 10H-, 12H-, 18H-SiC polytypes [26].

For example, the different percentage of hexagonality (h) for structures $10H_2$ ⟨55⟩ and $10H_1$ ⟨3223⟩ is shown in Fig. 7.

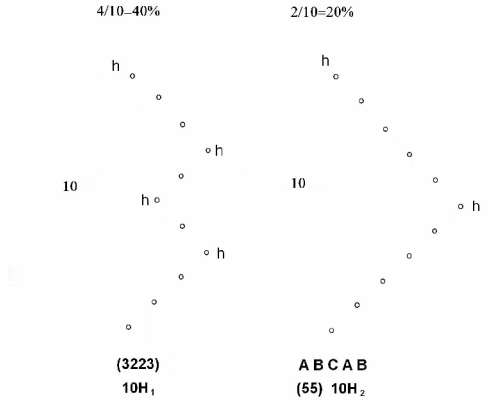

Fig. 7. Calculation of the hexagonality percentage for 10H – SiC.

Moreover, the motif of the metastable nano-scale building structures $10H_1$ ⟨3223⟩ (with 40% hexagonality) corresponds to the motive of building structure 15R ⟨$(32)_3$⟩, which takes place in stable conditions. The motif of $14H_1$ ⟨4334⟩ (28.5% h) corresponds to the known stable polytype 21R ⟨$(34)_3$⟩.

4. Conclusion

LTPL of pure α-SiC crystals and pure crystals of β-SiC are represented by the similar spectra of SFs, which are indicators of formation of the metastable nanostructures, namely: 14H1 ⟨4334⟩, $10H_2$ ⟨55⟩, $14H_2$ ⟨77⟩, 33R ⟨$(3332)_3$⟩, 8H ⟨44⟩.

Comprehensive spectroscopic studies revealed the same principle of construction and the same behavior of each of the SFs spectra under various external influences on the crystals. The difference in interlayer bond's energies for the exactly same structure of each layer gives appearance of the super-fine SF – I and SF – II parts of every SFs spectrum. All SFs spectra are observed within the temperature range 4.2 to 35 K (SF – I at 4.2…15 K, SF – II at 4.2…35 K). SF – I corresponds to radiation caused by atoms creating the V (hexagonal) bonds between layers, SF – II corresponds to radiation of atoms creating the N (cubic) bonds between layers. Spectroscopic data have shown the same principle and the same behavior of the construction of each SFs spectrum under different external influences on the crystals.

The results of this work have shown the mechanism of interfacial rearrangements, which allows monitoring the processes of transforming the energy states in the crystal.

References

1. I.S. Gorban and G.N. Mishinova, The bases of luminescent diagnostic of dislocation structure of SiC crystals// *Proc. SPIE*, **3359**, p. 187 (1998).
2. A. Galeckas, H.K. Nielsen, J. Linnros, A. Hallen, B.G. Svensson, and P. Pirouz, Investigation of stacking fault formation in hydrogen bombarded 4H-SiC // *Mater. Sci. Forum,* **483-485**, p. 327-330 (2005).
3. S.I. Maximenko, P. Pirouz, and T. Sudarshan, Investigation of the electrical activity of partial dislocations in SiC p-i-n diodes // *Appl. Phys. Lett.* **87**(3), 033503-0-033503-3 (2005).
4. A. Galeckas, and J. Linnros, P. Pirouz, Recombination induced stacking faults: Evidence for a general mechanism in hexagonal SiC // *Phys. Rev. Lett.* **96**(2), 025502-1-025502-4 (2006).
5. S.I. Maximenko, P. Pirouz and T.S. Sudarshan, Open core dislocations and surface energy of SiC // *Mater. Sci. Forum,* **527-529**, p. 439-442 (2006).
6. P. Pirouz, M. Zhang, H.McD. Hobgood, M. Lancin, J. Douin, and B. Pichaud, Nitrogen doping and

multiplicity of stacking faults in SiC // *Phil. Mag. A*, **86** (29-31), p. 4685-4697 (2006).
7. G. Regula, M. Lancin, H. Idrissi, B. Pichaud and J. Douin, Structural characterization of double stacking faults induced by cantilever bending in nitrogen-doped 4H-SiC // *J. Appl. Phys.* **101**(11), p. 113533.1-113533.5 (2007).
8. G.R. Fisher, P. Barnes, Toward a unified view of polytypism in silicon carbide // *Phil. Mag. B*, **61**(2), p. 217-236 (1990).
9. S.I. Vlaskina, D.H. Shin, 6H to 3C polytype transformation in silicon carbide // *Jpn. J. Appl. Phys.* **38**, p. L27-L29 (1999).
10. Shin Sugiyama, Motohiro Togaya, Phase relationship between 3C- and 6H-silicon carbide at high pressure and high temperature // *J. Amer. Ceram. Soc*. **84** (12), p. 3013-3016 (2001).
11. S.I. Vlaskina // *Semiconductor Physics, Quantum Electronics and Optoelectronics*, **5**(2), p. 252 (2002).
12. M. Durandurdu, Ab initio simulations of the structural phase transformation of 2H-SiC at high pressure // *Phys. Rev. B*, **75**, p. 235204 (2007).
13. S.W. Lee, S.I. Vlaskina, V.I. Vlaskin, I.V. Zaharchenko, V.A. Gubanov, G.N. Mishinova, G.S. Svechnikov, V.E. Rodionov, S.A. Podlasov, Silicon carbide defects and luminescence centers in current heated 6H-SiC // *Semiconductor Physics, Quantum Electronics and Optoelectronics*, **13**(1), p. 24-29 (2010).
14. C. Raffy, J. Furthmuller, F. Bechstedt, Properties of interfaces between cubic and hexagonal polytypes of silicon carbide // *J. Phys.: Condens. Matter*, **14**(48), p. 12725-12731 (2002).
15. A. Romano, J. Li, S. Yip, Atomistic simulation of rapid compression of fractured silicon carbide // *J. Nucl. Mater*. **352**, p. 22-28 (2006).
16. F. Shimojo, I. Ebbsjo, R.K. Kalia, A. Nakano, J.P. Rino, and P. Vashishta, Molecular-dynamics simulation of structural transformation in silicon carbide under pressure // *Phys. Rev. Lett.* **84**, p. 3338-3341 (2000).
17. F. Bechstedt, P. Kackell // *Phys. Rev. Lett.* **75**, p. 2180 (1995).
18. J.Q. Liu, M. Skowronski, C. Hallin, R. Soderholm and H. Lendenmann, Structure of recombination-induced stacking faults in high voltage SiC p-n junctions // *Appl. Phys. Lett.* **80**, p. 749 (2002).
19. M.S. Miao, S. Limpijumnong and W.R. Lambrecht, Stacking fault band structure in 4H SiC and its impact on electronic devices // *Appl. Phys. Lett*. **79**, p. 4360-4362 (2001).
20. S. Juillaguet, T. Robert, J. Camassel Optical investigation of stacking faults in 4H-SiC epitaxial layers: Comparison of 3C and 8H polytypes // *Mater. Sci. Eng. B – Solid State Mater. Adv. Technol.*, **165**, p. 5-8 (2009).
21. A. Bauer, P. Reischauer, J. Kräusslich, N. Schell, W. Matz and K. Goetz, Structure refinement of the silicon carbide polytypes 4H and 6H: unambiguous determination of the refinement parameters // *Acta Cryst. A*, **57**, p. 60-67 (2001).
22. B. Wen, J. Zhao, M. Bucknum, P. Yao, T. Li, First principles studies of diamond polytypes // *Diamond Relat. Mater.* **17**, p. 356-364 (2008).
23. F. Herman, J.P. van Duke, R.L. Kortum, Electronic structure and spectrum of silicon carbide // *Mater. Res. Bull.* **4**, p. S167-S178 (1969).
24. S. Shinozaki, K.R. Kisman, Aspects of "one dimensional disorder" in silicon carbide // *J. Acta Metallurgica*, **26**, p. 769-776 (1978).
25. L.U. Ogbuji, T.E. Mitchell, A.H. Heuer, The $\beta \rightarrow \alpha$ transformation in polycrystalline SiC // *J. Amer. Ceram. Soc.* **64**(12), p. 91-99 (1981).
26. Kazuaki Kobayashi, Shojiro Komatsu, First-principles study of 8H-, 10H-, 12H-, and 18H-SiC polytypes // *J. Phys. Soc. Jpn. Appl.* 024714 (2012).